IEEE/CSC & ESAS EUROPEAN SUPERCONDUCTIVITY NEWS FORUM (ESNF), No. 10, October 2009.
Published in *AIP Conference Proceedings* **1219**, pp. 208-215 (2010)

CONTACT MECHANICS MODEL FOR TRANSVERSE LOAD EFFECTS ON SUPERCONDUCTING STRANDS IN CABLE-IN-CONDUIT CONDUCTORS

L. Chiesa[1], M. Takayasu[2], and J. V. Minervini[2]

[1]Tufts University
Medford, MA, 02155, USA

[2]Massachusetts Institute of Technology
Cambridge, MA, 02139, USA

ABSTRACT

A new model based on contact mechanics concepts has been developed to analyze and quantitatively evaluate mechanical transverse load effects on superconducting strands in a cable-in-conduit-conductor (CICC). It has been used to determine the number of contact points and the effective contact pressures among the strands in a cable. The new model has been confirmed by experimental measurements and it is used to explain mechanical transverse load effects on the critical current degradation of sub-sized cable samples. The transverse load degradations of the critical currents of a large CICC cable can be evaluated based on experimental critical-current degradation data of a 3-strand cable as a function of the effective contact pressure. The model predicts the critical current degradations of cables like an ITER full size conductor as high as 20% caused solely by the transverse Lorentz load effect. Parametric studies performed with this model indicate that the initial degradation could be reduced by shortening the twist pitch length of the initial stages of a full size cable or by mechanically supporting the last stage bundles of the cable. This analysis shows that the transverse Lorentz load effect, which is inherent in the CICC design, contributes a significant fraction of the degradation of a large Nb_3Sn superconducting cable.

KEYWORDS: Contact mechanics, Cable-In-Conduit-Conductors (CICC), critical current, transverse stress, Nb_3Sn, superconducting cable.

INTRODUCTION

An experimental setup to study the transverse load effect on superconducting cables has been built and successfully tested as described in [1]. Three different hairpin samples, single strand, triplet and 45-strand cable, were tested with the setup and the data were used to develop a new model to evaluate effective transverse load in a Nb_3Sn cable.

The transverse load pressure due to the electromagnetic Lorentz force is often referred to as "averaged pressure" because it is determined from the force divided by the projected area of the sample cross-section. The averaged pressure does not take into account the actual area pressed and the local effects that might occur within the sample. In a cable composed of many strands, the real pressed contact area acting on a strand is a combination of the angle between crossing strands and the number of their contacts. Using the projected area of the wire or the cable is a very simplified way of estimating the pressure exerted on strands, and the averaged pressure can be much smaller than the actual pressure experienced by each strand caused by the local contacts with strands in a cable.

In this paper a model to evaluate the real deformation of the cables under a mechanical load is presented according to the theory of contact mechanics. The new model quantitatively evaluates the effective contact pressure between strands. This model predicts the number of contact points and the contact area between strands in a cable, and evaluates the transverse load effects on performances of superconducting cables. It is proposed to use a set of experimental transverse load test data of the smallest stage cable (triplet) to predict the performance of larger cables.

CONCEPTS OF CONTACT MECHANICS

When two bodies come in contact, stresses and deformation arise from the contact. Those quantities can be studied using contact mechanics. This theory has been developed first by Hertz in 1892 [2]. More details have been developed by Timoshenko, Goodier and Lessells [3-5] who presented derivation of elastic equations for loading of elastic half-spaces. The case studies most relevant to this paper are summarized in this section [6].

In TABLE 1, the equations used for the analysis are shown. The single strand of radius a is simulated with an external force F_c applied by two cylinders on both sides as shown in the table. The contact area is a rectangle surface. In the case of a contact between two strands, the contact area is an ellipse of semi-axis η and ξ. F_c is the transverse force for each contact. It is noted that the Young's modulus E is only unknown parameter in TABLE 1 and it is used as fitting parameter in our analysis. To analyze the contact pressure from the total force acting on a cable, the number of contact points needs to be evaluated as discussed later in the next section.

Applying a uniform transverse load on a single strand is very different from the type of interactions between strands in a cable which is wound in multiple stages with a 3-strand cable being typically the first stage configuration. The 3-strand cable configuration seems to be the basic representative of a larger cable.

FIGURE 1 (left) shows the calculated displacement compared with the experimentally measured one [1] for the 3-strand cable. A fair agreement is obtained for values of E of 3 GPa. In FIGURE 1 (right), the critical current results are plotted as a function of the contact pressure calculated from the equations in TABLE 1. In the figure the same critical current data are plotted with the conventional averaged pressure (diamond symbols) for comparison. The effective contact pressure values are much larger.

TABLE 1. List of equations used for the analysis. , α and β are tabulated values dependent on the crossing angles ϕ between the two solids [7-8].

	SINGLE STRAND	TWO-STRAND
	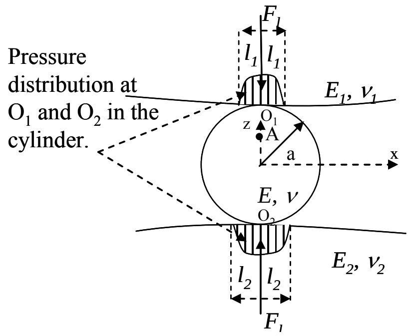	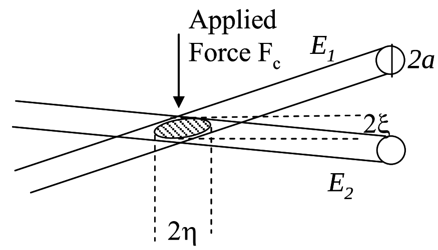
Effective contact area	$S_c = L \cdot 2l_i$	$S_c = \pi \cdot \eta \cdot \xi$
Characteristic dimension	$l_i^2 = 4 \cdot F_l \cdot R_{eq,i} /(\pi \cdot E_i^*)$	$\eta = \alpha \cdot \left(F_c \cdot K_D / E^*\right)^{1/3}$ $\xi = \beta \cdot \left(F_c \cdot K_D / E^*\right)^{1/3}$
Displacement	$\delta_s = 2F_l \cdot \frac{1-\nu^2}{\pi \cdot E} \cdot \left\{ \ln\left(\frac{4a}{l_1}\right) + \ln\left(\frac{4a}{l_2}\right) - 1 \right\}$	$\delta_x = \lambda \cdot \sqrt[3]{F_c^2 /((E^*)^2 \cdot K_D)}$
Effective contact pressure	$p_l = F_l / 2l_i$	$p_c = F_c / S_c$
Other quantities	$1/E_i^* = (1-\nu^2)/E + (1-\nu_i^2)/E_i$ $1/R_{eq,i} = 1/a + 1/R_i$	$1/E_i^* = 2(1-\nu^2)/E$ $K_D = 3a/4$

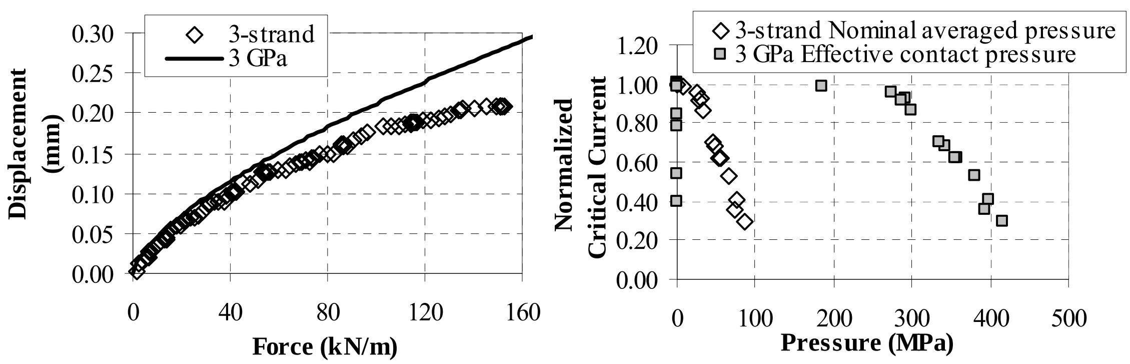

FIGURE 1. Transverse displacement (measured and calculated) as a function of force per unit length for the 3-strand sample (left). Calculated curve is for E = 3 GPa. Critical current as a function of contact pressure obtained with E = 3 GPa for the 3-strand sample (right). The same critical current data are plotted with the nominal averaged pressure.

NUMBER OF CONTACTS IN A CABLE

The number of strand-to-strand contacts is calculated for the different stages starting from a 3-strand cable. In general a cable-in-conduit conductor is produced in multiple stages starting from twisting three strands (triplet) together and then twisting together three or four bundles and so on, until the final stage is reached. When a transverse load is applied to a 3-strand cable it is noted that there are six places of strand-to-strand contact points that support the load in one twist pitch length as shown in FIGURE 2. At each contact, two strands overlap each other to make one strand-to-strand contact, so that the total number of strand-to-strand contacts is 6 per twist pitch, which is twice the number of strands composing the cable. The next stage could be composed of three, four or five bundles of 3-strand cables (3x3, 3x4, 3x5). FIGURE 3, for example, shows the 5-bundles case. In the case of five bundles the number of bundle-to-bundle contact places is 10. In general, the contact places between sub-bundles are given by $2 \cdot k$ where k is the number of bundles.

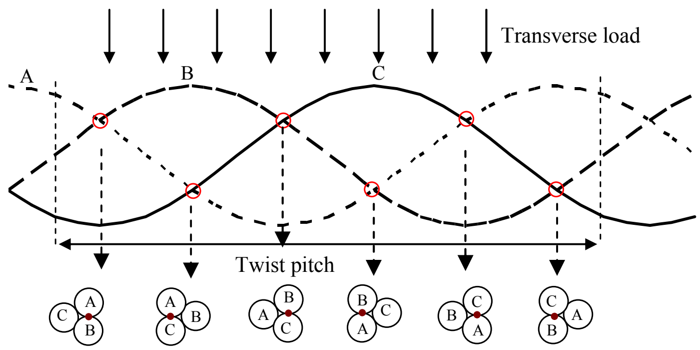

FIGURE 2. Triplet under transverse load and contact places in one twist pitch length.

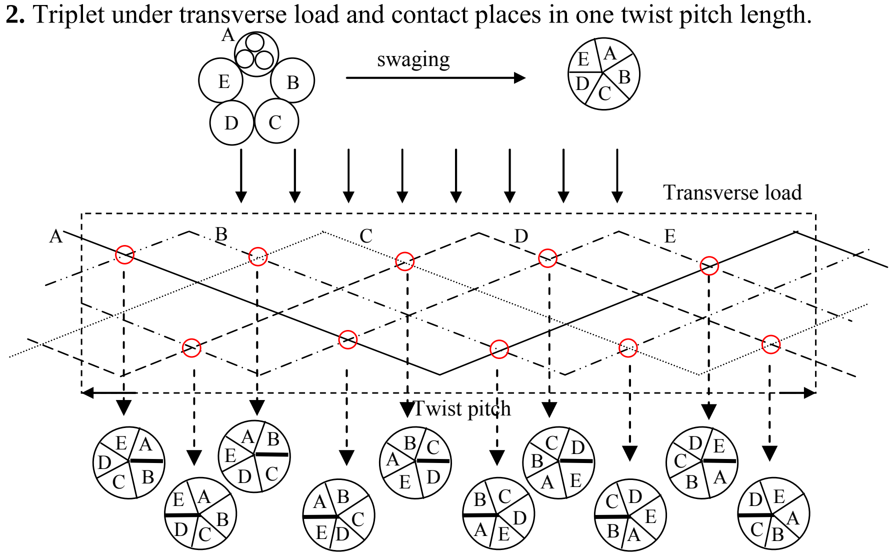

FIGURE 3. Five-bundle cable under transverse load and contact places in one twist pitch length.

The approach followed with the examples just presented allows concluding that the bundle crossing contact places, $N_{cross,i}$, for the stage i, where the strand-to-strand contact points are created after cable swaging, is given per unit length by equation 1:

$$N_{cross,i} = 2 \cdot k_i / L_{p_i} \tag{1}$$

where k_i is the number of bundles and L_{pi} is the twist pitch for stage i.

To evaluate the total number of strand-to-strand contact points at the bundle crossing contact place, it is necessary to determine the number of strands in the bundle-to-bundle contact. The strand-to-strand contacts occur between bundles as illustrated in FIGURE 4. The width of the bundle-to-bundle contact at the bundle crossing contact place in a swaged cable can be taken to be equal to the radius of the cable as shown in the figure. The strand-to-strand contacts N_i of stage i of a cable composed of a total number of strands N_{si} is given per unit length as:

$$N_i = 2 \cdot k_i \cdot n_{Ri}^{\,2} / L_{pi} = 2 \cdot k_i \cdot 4 \cdot (1 - \nu_f) \cdot \cos\vartheta \cdot N_{si} / (\pi^2 \cdot L_{pi}) \tag{2}$$

with all the relevant parameters defined in TABLE 2.

TABLE 2. Quantities necessary to evaluate equation (2).

Total number of strands for a *i*-stage cable. $N_{si} = k_1 \cdot k_2 \cdot \ldots \cdot k_i$ (3)	k_i is the number of bundles in the stage *i*.
Radius of cable (FIGURE 4). $R = \sqrt{\dfrac{N_s \cdot a^2}{(1-v_f) \cdot \cos\vartheta}}$ (4)	N_s is the total number of strands, a the radius of a single strand, v_f the void fraction of the cable and θ is the average angle between strands and the cable axis. For a large cable like the ITER cable $\cos\theta$ is 0.93-0.95 and θ is 15-20°. For smaller cables $\cos\theta > 0.99$ so that it does not have to be taken in consideration in the calculations.
Number of strands across the radius *R*. $n_{Ri} = 2(1-v_f)\cos\vartheta \cdot R/(\pi \cdot a)$ (5)	Both bundles expose the same amount of strands to the contact area as illustrated in FIGURE 3, so that the cross contact points are given by n_{Ri}^2 (for stage *i*).

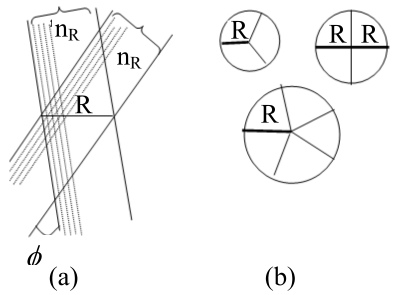

FIGURE 4. (a) Schematic view of the crossing contact between bundles. (b) Cross-section views of three, four and five-bundle cables swaged.

MODELING OF CRITICAL CURRENT BEHAVIOR

Transverse loads are caused by an external mechanical load and an electromagnetic Lorentz load due to the self current and field. There is a fundamental difference between these two approaches. The external mechanical load is applied uniformly through the cross section of a cable, while the Lorentz load accumulates through the cross section (FIGURE 5). The model takes in consideration these two different scenarios to evaluate transverse load effects on the critical current in a cable. The critical current of a particular strand depends on the contact force acting on the strand. In the case of the external mechanical load the force in each horizontal plane is the same. Each strand in a horizontal plane experience the same contact force (the transverse load divided by the number of contacts in a plane perpendicular to the load). On the other hand the contact force due to the Lorentz force will depend on the location of the strand in the cable (the force on layer A depends on the current distribution and force accumulation of the layers above). The number of strand-strand contacts and their distribution in a cable are the same in both cases.

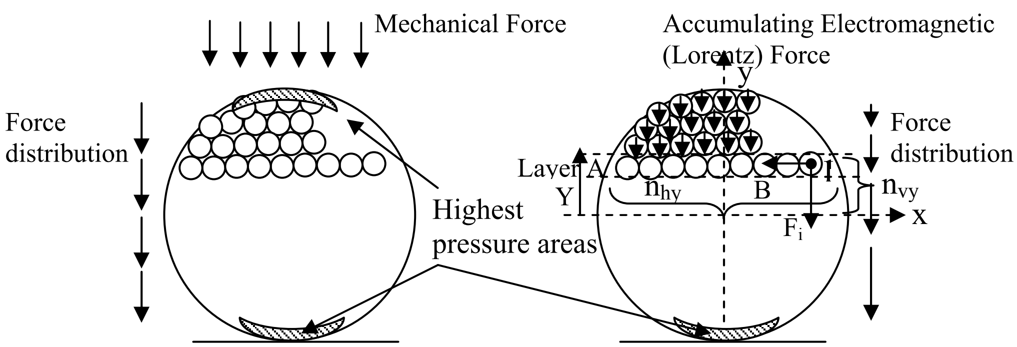

FIGURE 5. Force configuration for a cable loaded with an external mechanical load (left) and the accumulation of a natural Lorentz load (right).

TABLE 3. Quantities necessary to evaluate equation (10).

Lorentz force per unit length caused by strands in a layer A at position y = Y. $\Delta f_{LFy} = B \cdot I_0 \cdot n_{hy} \cdot \frac{N_{sc}}{N_s} \cdot \frac{\Delta y}{2 \cdot a} = B \cdot 2 \cdot (1-v_f) \cdot \cos\vartheta \cdot \sqrt{R_{cable}{}^2 - y^2} \cdot N_{sc} / N_s \cdot (I_{c-single}(p_{cy}) / \pi \cdot a^2)\Delta y$	(6)	B is the magnetic field, and $I_{c\text{-}single}(p_{cy})$ is the critical current of a single strand at a certain contact pressure p_{cy}.
Number of strands on a horizontal plane at height *y*. $n_{hy} = 2 \cdot (1-v_f) \cdot cos\vartheta \cdot \sqrt{(R_{cable}{}^2 - y^2)} \cdot 2a / \pi \cdot a^2$	(7)	The Lorentz force is vertical (FIG. 5).
Number of the strand-to-strand contact points in a plane per unit length. $N_{hy} = (N_T / N_s) \cdot n_{hy}$ $N_T = k_2 \cdot k_3 \cdot k_4 \cdot k_5 \cdot N_1 + k_3 \cdot k_4 \cdot k_5 \cdot N_2 + k_4 \cdot k_5 \cdot N_3 + k_5 \cdot N_4 + N_5$	(8)	N_T is the total contact points in a cable per unit length (found using N_i from equation 3). v_f is the void fraction, R_{cable} the cable radius, a the strand radius and θ is the average angle between strand and cable axis.
$\cos\vartheta = N_s A_{strand} / A_{cable}(1-v_f)$	(9)	

In the case of the Lorentz load, the total transverse force acting on a horizontal plane layer A at location Y, F_{LFy}, caused by the strands above the layer A strands and the layer-A strands, can be written as:

$$F_{LFy} = \int_Y^{R_{cable}} \Delta f_{LFy} = \frac{2 \cdot B \cdot N_{sc}}{\pi \cdot a^2 \cdot N_s} \cdot (1-v_f) \cdot cos\vartheta \int_Y^{R_{cable}} I_{c-single}(p_{cy}) \cdot \sqrt{R_{cable}{}^2 - y^2}\, dy \tag{10}$$

where all the quantities are defined in TABLE 3 for a 5-stage cable taken as example. The function $I_{c\text{-}single}(p_{cy})$ is the critical current as a function of the contact pressure p_{cy}. The transverse load effect on the critical current can be obtained from an experiment of a triplet. The contact pressure p_{cy} is the ratio of the contact force F_{cy} on a strand at a particular location y, divided by the contact area S_c ($p_{cy}=F_{cy}/S_c$). The contact force F_{cy} is the ratio of the force acting on a layer divided by the contact points in the layer ($F_{cy}=F_{LFy}/N_{hy}$).

The normalized critical current I_c^* of the cable as a function of load can be written for an untwisted and fully twisted cable respectively as:

Untwisted
$$I_c^* = \frac{I_c}{I_{c0}} = \frac{2}{\pi \cdot a^2 \cdot N_s} \int_{-R_{cable}}^{R_{cable}} I^*_{c-single}(p_{cy}) \cdot (1-v_f) \cdot cos\vartheta \cdot \sqrt{(R_{cable}{}^2 - y^2)}\, dy \tag{11}$$

Fully twisted
$$I_c^* = \frac{I_c}{I_{c0}} = \frac{2 \cdot \pi \cdot (1-v_f) \cdot cos\vartheta}{N_s \cdot \pi \cdot a^2} \int_{-R_{cable}}^{0} I^*_{c-single}(p_{cy}) \cdot y\, dy \tag{12}$$

In the case of a fully twisted cable each strand is assumed to spiral along the cable axis, and in a twist pitch length it will go back to its original location. In a twist pitch length, each strand will experience the highest Lorentz load at some point so that the currents of strands on the same annulus will transport the same current *I(r)* corresponding to the minimum critical current experienced in a twist pitch length. No current sharing among strands is assumed in a twist pitch length (true for a chrome plated wire cable).

The integrals in equations (11) and (12) are evaluated using Gaussian integration. It is calculated using Microsoft Excel®. To evaluate the contact pressure p_{cy}, the strand currents are required so an iteration process was used to perform the critical current calculations.

In the case of the external mechanical force, the normalized critical current, I_c^*, has the same expressions as equations (11) and (12) but the distribution of the contact pressure p_{cy} is different from that of the Lorentz force case.

MODEL RESULTS

The critical current of fully twisted cable, equation (12), allows simulating superconductor performances of various CICC cables. For the model analysis, the critical current behavior $I^*_{c\text{-}single}(p_{cy})$ on the transverse pressure for a given wire is required to evaluate equation (12). In the following analyses the experimental $I^*_{c\text{-}single}(p_{cy})$ obtained at the background field of 12 T for the 3-strand sub-cable experiment of Oxford ITER pre-production Nb_3Sn wire was used, and 3 GPa was used as Young's modulus [1]. We disregard the variation of magnetic fields across the cross section of the cable. The purpose of the model analyses is to have a general idea of the effects of transverse load.

The model results show that for a full size cable with the original cable pattern proposed for the TF coil in ITER (cabling pattern 3x4x4x4x6 and twist pitches 65, 90, 150, 270, 430 mm), the Lorentz load could account for up to 20% of degradation as shown in FIGURE 6 (left). To reduce the degradation caused by the transverse Lorentz load each sub-cable could be supported. For example, if the 6 petals of the last stage of the TF cable are independently supported (each one carrying 11.6 kA), the degradation would be 6% (FIGURE 6 right plot). Cabling patterns and twist-pitches of cabling mitigate the effect of the transverse load as shown in FIGURE 7. Lower number of bundles in a stage causes higher degradation in general. A cabling pattern 3x3x3x3x6 shows a 10% larger degradation than a cabling pattern 3x5x5x6 (left). Shorter twist pitches at the first stage are preferable (right).

Tests performed on full size magnets (TFMC, TFI, CSMC, CSI) showed unexpected initial degradation (50% TFMC, 35% CSI, TFI, 25% CSMC) [9]. Our model shows that the Lorentz load effect is one significant player in the degradation, showing 30% degradation at operational current of 80 kA for the TFMC.

It is important to stress the fact that the presented model takes into account only the degradation caused by the transverse contact pressure due to the Lorentz load. Axial and bending strains caused by thermal contractions and by the Lorentz load could be additional sources of the degradation, and can affect the performance of superconducting strands and of a full size cable, as discussed in [10-12]. Those effects are complementary and not mutually exclusive so all should be considered in the overall performance of a cable. The work reported in this paper was limited to the contact pressure effect due to transverse load.

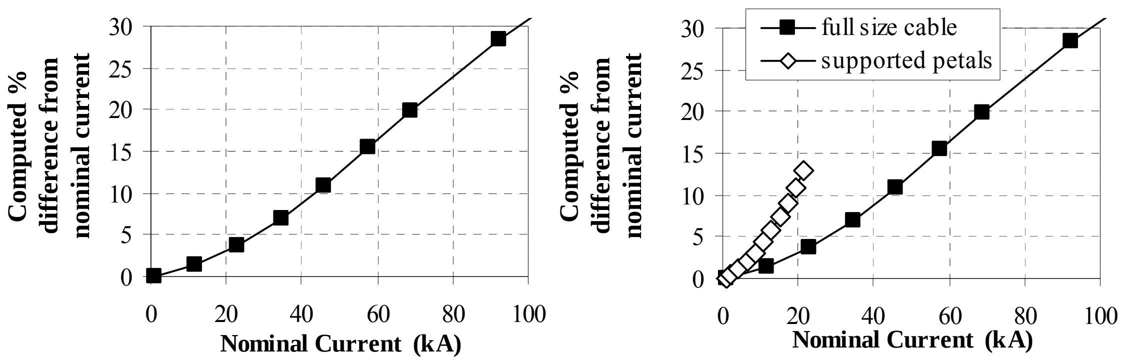

FIGURE 6. Percent differences between the nominal current and the expected values considering the natural Lorentz load effect for the proposed TF cable configuration 3x4x4x4x6 (left). Comparison with a cable with independently supported petals (right).

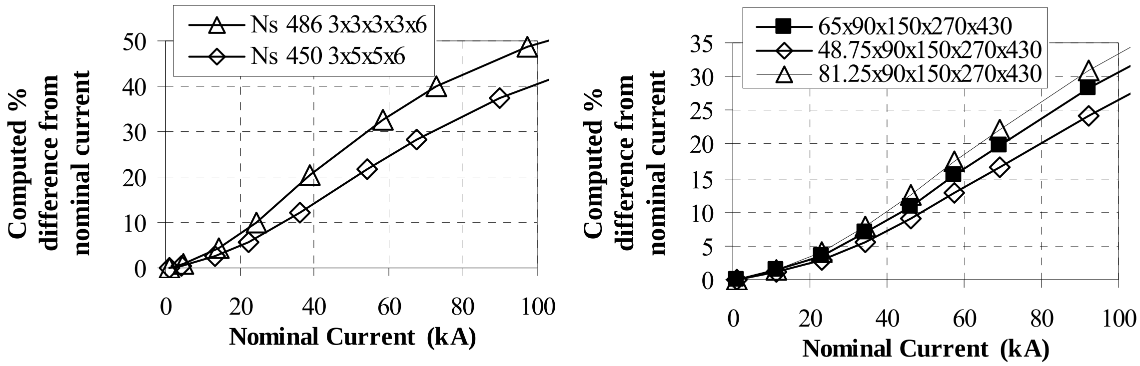

FIGURE 7. Percent differences between the nominal current and the expected values considering the Lorentz load effect for a cable with different cabling pattern (left) and twist pitch configurations (right).

CONCLUSIONS

A new model based on contact mechanics between strands was presented to explain the transverse load degradation. A method evaluating quantitatively the number of contacts and the effective contact pressure between strands has been developed. With experimental support, it has been proposed to use the 3-strand transverse-load performance data of the critical current to simulate the degradation of a large full size cable due to Lorentz load effect.

For the first time the contact pressure Lorentz load effect is quantitatively shown to be a significant fraction of the inherent degradation of a large Nb_3Sn superconducting cable. To reduce the degradation caused by the transverse Lorentz load, higher number of bundles in a stage, shorter twist pitches, and supported sub-cables could be used. It has to be noticed that for the overall degradation of a cable other sources such as axial and bending strains need to be considered.

The model presented needs to be verified with more experimental work by using different cabling parameters (twist pitch, cable pattern, and wire diameter) to investigate how to improve and optimize a cable design.

ACKNOWLEDGEMENTS

This work was supported by the U.S. Department of Energy, Grant No. DE-FC02-93ER54186. A portion of this work was performed at the National High Magnetic Field Laboratory, which is supported by NSF, the State of Florida and the DOE.

REFERENCES

1. L. Chiesa et al., presented at this conference, section M3-B-02, CEC-ICMC 2009.
2. H. Hertz, "*Miscellaneous papers*", Macmillan and Co., New York 1896.
3. S.P. Timoshenko, J.N. Goodier, "*Theory of Elasticity*", 3rd edition, McGraw-Hill Book, 1970.
4. S.P. Timoshenko, J.M. Lessells, "*Applied Elasticity*", Westinghouse Tech. Night School Press, 1925.
5. S.P. Timoshenko, "*Strength of Materials*", Van Nostrand Reinhold Company.
6. K.L. Johnson, "*Contact Mechanics*", Cambridge University Press, 1985.
7. H.L. Whittemore and S.N. Petrenko, Technical Paper of the Bureau of Standards #201, 1921.
8. M. Kornhauser, *Journal of Applied Mechanics*, vol. **18**, p. 251-252 (1951).
9. N. Martovetsky, *Physica C* **401** (2004) 22–27.
10. N. Mitchell, *Fusion Engineering and Design*, Vol. **66–68**, p. 971–993, 2003.
11. A. Nijhuis, *Supercond. Sci. Technol.* **21**, 2008.
12. Y. Zhai and M. Bird, *Supercond. Sci. Technol.* **21**, 2008.